The arm was initially placed in the vertical equilibrium configuration

$$\theta = (-90 \quad 0)^T \text{ [deg]} \quad \delta = (0 \quad 0 \quad 0 \quad 0)^T \text{ [m]}.$$

The desired joint configuration was chosen

$$\theta_{\text{des}} = (-45 \quad 0)^T \text{ [deg]}.$$

From (9), with the above values of stiffness coefficients, the residual deflections at the desired state were computed as

$$\delta_{\text{des}} = (-0.15 \quad -0.0045 \quad -0.0056 \quad -0.000076)^T \text{ [m]}.$$

The PD feedback gains were chosen as

$$K_P = \text{diag}(18, 18)\text{[Nm/rad]}$$
$$K_D = \text{diag}(10, 2)\text{[N m s/rad]}.$$

The resulting arm behavior under the PD+ control (8) is described by the plots in Fig. 2. It is easy to see that the desired state $(\theta_{\text{des}}, \delta_{\text{des}})$ is asymptotically reached, well within 2 s. Notice the large control effort at the start of the motion and the constant torques resulting at steady-state so as to compensate for gravity. The simulations also revealed the following facts.

- We computed a value for α in (6) a posteriori for the simulated trajectory, obtaining $\alpha = 17.67$; thus, both conditions (14) and (15) are actually satisfied. Indeed, those conditions are only sufficient, and we achieved satisfactory results even for smaller values of proportional gains.
- When increasing the gains, the system remained stable at the expense of high initial torques though. We observed, however, that too large values caused numerical instabilities, especially in association with large initial errors. A typical remedy for this inconvenience would be to impose an interpolating trajectory from the initial to the desired state even if the required motion is a point-to-point task.
- We verified that the nonlinear control law (30) leads to very similar results, not reported here for brevity; in particular, it was found that the initial control effort is reduced in view of the gravity compensation performed for the actual system configuration.

References

[1] S. Arimoto and F. Miyazaki, "Stability and robustness of PID feedback control for robot manipulators of sensory capability," in *Robotics Research: 1st Int. Symp.*, M. Brady and R. P. Paul, Eds. Cambridge, MA: MIT Press, 1984, pp. 783–799.

[2] P. Tomei, "Adaptive PD controller for robot manipulators," *IEEE Trans. Robotics Automat.*, vol. 7, pp. 565–570, 1991.

[3] P. Tomei, "A simple PD controller for robots with elastic joints," *IEEE Trans. Automat. Contr.*, vol. 36, pp. 1208–1213, 1991.

[4] A. De Luca and B. Siciliano, "Relevance of dynamic models in analysis and synthesis of control laws for flexible manipulators," in *Robotics and Flexible Manufacturing Systems*, S. G. Tzafestas and J. C. Gentina, Eds. Amsterdam: Elsevier, 1992, pp. 161–168.

[5] L. Lanari and J. T. Wen, "Asymptotically stable set point control laws for flexible robots," *Systems & Control Lett.*, vol. 19, pp. 119–129, 1992.

[6] H. G. Lee, S. Arimoto, and F. Miyazaki, "Liapunov stability analysis for PDS control of flexible multi-link manipulators," in *Proc. 27th IEEE Conf. Decision Contr.*, Austin, TX, 1988, pp. 75–80.

[7] W. J. Book, "Recursive Lagrangian dynamics of flexible manipulator arms," *Int. J. Robotics Res.*, vol. 3, no. 3, pp. 87–101, 1984.

[8] A. De Luca and B. Siciliano, "Closed-form dynamic model of planar multi-link lightweight robots," *IEEE Trans. Syst., Man, Cybern.*, vol. 21, pp. 826–839, 1991.

[9] S. Cetinkunt and W. L. Yu, "Closed-loop behavior of a feedback controlled flexible arm: a comparative study," *Int. J. Robotics Res.*, vol. 10, pp. 263–275, 1991.

[10] W. Hahn, *Stability of Motion.* Springer Verlag, Berlin, 1967.

[11] L. Meirovitch, *Analytical Methods in Vibrations.* New York: Macmillan, 1967.

[12] K. H. Low, "Solution schemes for the system equations of flexible robots," *J. Robotic Syst.*, vol. 6, pp. 383–405, 1989.

[13] T. E. Alberts, "Augmenting the control of a flexible manipulator with passive mechanical damping," Ph.D. dissertation, School Mech. Eng., Georgia Inst. Technol., Atlanta, GA, 1986.

Control of Flexible Arms with Friction in the Joints

Vicente Feliu, Kuldip S. Rattan, and H. Benjamin Brown, Jr.

***Abstract*— The control of flexible arms with friction in the joints is studied. A method to identify the dynamics of a flexible arm from its frequency response (which is strongly distorted by Coulomb's friction) is proposed. A robust control scheme that minimizes the effects of this friction is presented. The scheme consists of two nested feedback loops: an inner loop to control the motor position and an outer loop to control the tip position. It is shown that a proper design of the inner loop eliminates the effects of friction while controlling the tip position and significantly simplifies the design of the outer loop. The proposed scheme is applied to a class of lightweight flexible arms, and the experiments show that the control scheme results in a simple controller. As a result, the computations are minimized and, thus, high sampling rates may be used.**

I. Introduction

A major research effort has been made in the last five years to control flexible structures and, in particular, flexible arms. Several papers have appeared on this topic studying different aspects: Cannon and Schmitz [1] and Matsuno *et al.* [2] are examples of controlling the endpoint position using state-space techniques; Harahima and Ueshiba [3], Siciliano *et al.* [4], and Rovner and Cannon [5] used different adaptive control schemes to account for changes in the load; and Ower and Van de Vegte [6] used classical frequency-domain techniques to control a two-degree-of-freedom flexible arm. However, very little effort has been devoted to the control of flexible arms when static and dynamic frictions are present in the joints, although this is common in practice. The effects of friction are especially important in very lightweight, flexible arms or in flexible arms moving at low speeds and accelerations.

Several methods have been proposed to minimize the effects of friction in the control of dc motors. The simplest method uses a high-gain linear feedback. This method is based on the well-known property that the robustness of a closed-loop system to perturbations and changes in its parameters may be improved by increasing the

Manuscript received February 13, 1991; revised March 31, 1992. A portion of this work was presented at the 19th Annual Modeling and Simulation Conference, Pittsburgh, PA, May 1988, and the NASA-Air Force Workshop on Space Operations Automation and Robotics, Dayton, OH, July 1988.

V. Feliu is with the Department Ingenieria Electrica, Electronica y de Control, E.T.S.I. Industriales de la UNED, Madrid, Spain.

K. S. Rattan is with the Department of Electrical Engineering, Wright State University, Dayton, OH 45435.

H. B. Brown, Jr., is with the Robotics Institute, Carnegie-Mellon University, Pittsburgh, PA 15213.

IEEE Log Number 9207372.

open-loop gain [7]. Wu and Paul [8] used this method to compensate for friction in rigid arms, but its main limitation is that nonlinearities dominate any linear compensation for small errors and, therefore, result in small permanent errors in positioning. A more significant limitation appears when this method is applied to the control of flexible arms because most flexible arms are typically nonminimum phase systems (zeros in the right half-plane). This means that the controlled system becomes unstable if a high-gain loop is closed in order to control the tip position, making this method unsuitable. Another method for compensating friction is the use of force sensors and the mechanization of a feedback loop around the torque motor (see, for example, [9] and [1]; the latter is specifically for flexible arms). Finally, other methods are based on the use of a calculated compensation term added to the current of the motor to compensate for the friction torque such as Walrath [10], who used a model of the friction to predict its value and, more recently, Canudas *et al.* [11] who used a parameter identification procedure (a recursive least squares algorithm) to obtain this term.

Identification and control of flexible arms with friction in the joints is also studied herein. First, a new method to identify the dynamics of a flexible arm in the presence of Coulomb friction is presented in Section II. This method also provides an estimate of the average value of Coulomb friction over the range of working velocities. A new general control scheme that reduces the effects of friction is proposed in Section III. Existing methods to control flexible arms are based on explicit control of the tip position. In these schemes, the controller generates a control signal that is the current (after being properly amplified) for the dc motor that drives the arm. The proposed method is based on the simultaneous control of the joint motor position and tip position, and the implementation of two nested closed loops: an inner loop that controls the motor position and another outer loop that controls the tip position. In our scheme, the tip position is controlled by using the motor position instead of the current as a control signal. This is developed in Section III.

Section IV is devoted to the design of the inner loop controller. Compensation of Coulomb friction and the coupling torque between the motor and the beam is carried out. The purpose of this inner loop is to minimize the effects of frictional nonlinearities on the control system. The outer loop is designed in Section V according to classical control methods and combines feedforward–feedback controllers to accurately position the tip of the arm.

The proposed method is applied in Section VI to a class of one-link lightweight flexible arms that we have designed in our laboratory for experimental purposes. These lightweight arms are capable of performing quick movements. For these arms, the friction torque is comparable to the coupling torque between the motor and the beam, precluding the use of existing identification and control methods. Experimental results are given for two of these arms.

II. Identification

Frequency methods have been used extensively to identify the linear dynamics of flexible arms [1], [5], [12] because they allow a characterization of resonant frequencies. However, these methods were used in arms without friction in the joints. These methods can be extended easily to the case of linear dynamic friction, but give erroneous results when nonlinear Coulomb friction is present.

In this section, frequency identification techniques are modified to deal with nonzero Coulomb friction. In the following, we assume that the dynamics of the joint is given by

$$Ki(t) = J\frac{d^2\theta_m(t)}{dt^2} + V\frac{d\theta_m(t)}{dt} + C_t(t) + C_f(t) \qquad (1)$$

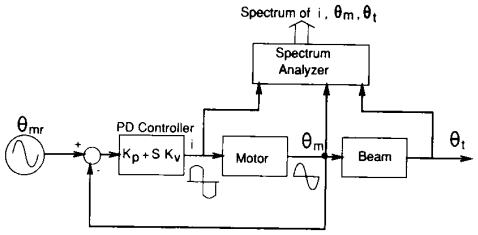

Fig. 1. Identification setup.

where K is the electromechanical constant of the motor, i is the current of the motor, θ_m is the motor position, J is the polar moment of inertia of the motor and hub, V is the dynamic friction coefficient, $C_t(t)$ is the coupling torque between the motor and the beam, $C_f(t)$ is the Coulomb friction torque, and t is the time. The coupling torque $C_t(t)$ is related to the angle $\theta_m(t)$ by a linear differential equation (it can be seen easily that there exists a transfer function between these two variables). The term $C_t(t)$ is related to the angular position and velocity of the motor.

Several models have been proposed to describe the friction of a dc motor, taking into account its linear and nonlinear terms (a review may be found in Canudas *et al.* [11]). Of these terms, Coulomb friction is the most important. This is especially true when dealing with direct-drive arms because the range of motor speed is relatively low and, consequently, dynamic friction is also low. Dynamic friction may be modeled in a first approximation by a linear term proportional to the speed of the motor, and Coulomb friction by a constant whose sign changes with the sign of the velocity of the motor. Thus we use the following friction model:

$$\text{Friction torque} = \begin{cases} C_f + V\dfrac{d\theta_m(t)}{dt}, & \text{if } \dfrac{d\theta_m(t)}{dt} > 0 \\ -C_f + V\dfrac{d\theta_m(t)}{dt}, & \text{if } \dfrac{d\theta_m(t)}{dt} < 0. \end{cases}$$

This simple model is a reasonable approximation of friction in many cases. Our identification method uses this model and provides an average value of all the parameters (either friction or linear dynamic parameters) of the arm because it is based on the spectral characteristics of the input and output signals.

Our method is divided in three stages [13]. First, a high-gain position loop is mechanized around the motor to make it follow the reference position closely. The achievement of this allows us to determine the velocity of the motor and, hence, the shape of the Coulomb friction. The magnitude of the Coulomb friction is then obtained from this shape and the spectral analysis of the measured signals. Finally, this value is used to correct the experimental measures of the frequency response of the motor that are distorted by this nonlinear friction term.

A. Control of Motor Position

First, a closed-loop control system for the motor position has to be designed to force the motor to follow a specified trajectory. The design of this controller is straightforward, and a standard proportional-plus-derivative (PD) controller may be used for this purpose. If a sinusoidal reference trajectory is applied to the closed-loop system, the angular velocity of the motor will be approximately sinusoidal. The motor current will reflect both the torque needed to accelerate the motor and the torque needed to overcome Coulomb friction, which is, ideally, a square wave in phase with the velocity of the motor. The magnitude of the Coulomb friction remains to be determined. The block diagram of the identification setup is shown in Fig. 1.

B. Calculation of the Magnitude of Coulomb Friction

Assume that the closed-loop position control system for the motor is excited by a sinusoidal reference signal of frequency ω_0. If the system were linear, we would find that the current and the angle of the motor would be sinusoids of the same frequency. However, because of the system nonlinearity, the current will not be sinusoidal. On performing a spectral analysis of the position and current signals [14], we find that: 1) the motor position response has only a peak at frequency ω_0, 2) the motor current has a dominant peak at frequency ω_0, and other peaks of smaller magnitude at frequencies $3\omega_0, 5\omega_0, 7\omega_0$, etc. This last phenomenon is explained by the Fourier series expansion of the Coulomb friction torque, which is represented by a square wave of frequency ω_0:

$$C_f(t) = \sum_{i=1}^{\infty} A_i \cos(i\omega_0 t); \qquad A_i = \frac{2C_f}{i\pi}(1 - (-1)^i), \quad (2)$$

where C_f is the magnitude of the Coulomb friction torque. According to (2), Coulomb friction generates odd harmonics of the fundamental frequency ω_0 that are part of the motor current (1) (θ_m only has the fundamental frequency).

We can now determine the magnitude of C_f, based on (2) and the study of the third harmonic. If the system is excited by a sinusoidal reference signal of frequency ω_0, then the fundamental component of the current is given by (1):

$$i_1(\omega_0) = G^{-1}(\omega_0)\theta_m(\omega_0) + \frac{4C_f}{K\pi} \exp\left[j\left(\frac{\pi}{2} + \angle\theta_m(\omega_0)\right)\right], \quad (3)$$

where $i_1(\omega_0)$ is the polar representation of the first harmonic of the current at ω_0, and $G^{-1}(\omega_0)$ is the frequency characteristic function of the linear part of the model of the motor (which includes motor-beam coupling torque) at frequency ω_0. Notice that the exponential term on the right side of this equation expresses the fact that Coulomb friction leads the position by 90°; that is, it is in phase with the velocity of the motor. Also with the system driven at ω_0, the third harmonic of the current is given by

$$i_3(3\omega_0) = G^{-1}(3\omega_0)\theta_{m3}(3\omega_0) + \frac{4C_f}{3K\pi} \exp\left[j\left(\frac{\pi}{2} + \angle\theta_m(\omega_0)\right)\right]. \quad (4)$$

Although $\theta_{m3}(3\omega_0)$ is close to zero in arms without any flexibility, that is not the case in flexible arms. When $3\omega_0$ is close to one of the natural frequencies of the beam, the position control system is unable to compensate completely for the varying beam torque due to the oscillations excited at that frequency. In this case the control system eliminates these oscillations sufficiently to consider that the motor position still closely follows a sinusoid of frequency ω_0, making (2) approximately valid. However, the high-frequency ripple that θ_m now contains, although small, should be considered in (4) because the factor $G^{-1}(3\omega_0)$ is very high [$G(j\omega_0) = 0$ at the beam resonant frequencies].

This experiment is repeated using a sinusoidal signal of frequency $3\omega_0$ as reference for the motor position. The fundamental component of the current is now

$$i_3(3\omega_0) = G^{-1}(3\omega_0)\theta_m(3\omega_0) + \frac{4C_f}{K\pi} \exp\left[j\left(\frac{\pi}{2} + \angle\theta_m(3\omega_0)\right)\right]. \quad (5)$$

Equations (4) and (5) constitute a system of two complex equations with two unknown complex parameters: $G(3\omega_0)$ and C_f. The value of C_f should be real in theory but, because of errors in measurements, it was found to have a small imaginary component. To get the real number C_f that gives the best approximation for (4) and (5), an algorithm that minimizes the following cost function was implemented.

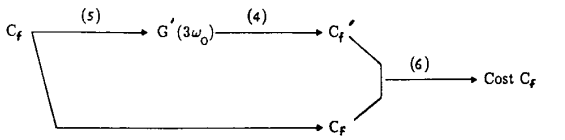

Fig. 2. Scheme for cost calculation.

$$\text{Cost} = (\ln(|C_f'/C_f|))^2 + (\angle C_f')^2, \quad (6)$$

where C_f' is defined from C_f in two steps: 1) for a given value of the Coulomb friction C_f, obtain $G'(3\omega_0)$ from (5); 2) from this value of G', obtain C_f' from (4). Then a function is defined between C_f and its associated cost according to Fig. 2.

The value of C_f that minimizes this cost function was obtained using a simple direct search method. Note that (6) represents the magnitude of the ratio $\ln(C_f'/C_f)$, which is a complex number. This cost function was chosen to give equal weights to errors in magnitude and phase.

It is convenient to repeat this procedure for different values of ω_0, and take the average among the resulting values of C_f as the estimation of the Coulomb friction. This is because the values of C_f may differ considerably depending on ω_0: We had variations of 20% around the mean value in our experiments.

C. Correction of Frequency Data

Once the mean value of the Coulomb friction is obtained, the frequency response of the linear part of the model of the motor $G(\omega)$ can be found from (3) by

$$G(\omega) = \frac{\theta_m(\omega)}{i(\omega) - (4C_f/K\pi)\exp\left[j\left(\frac{\pi}{2} + \angle\theta_m(\omega_0)\right)\right]}. \quad (7)$$

This expression is calculated using the experimental data obtained previously for the current $i(\omega)$ and the angle of the motor $\theta_m(\omega)$.

After obtaining the corrected experimental frequency data and an average value for the Coulomb friction, a transfer function may be fitted to these data by any of the existing methods. This transfer function gives the relationship between the current and the angle of the motor. Also obtained from the experimental data is the transfer function between the angle of the motor and the angle of the tip. Note that this way of representing the dynamics of the system is radically different from the way used in other approaches, in which relations between current and angle of the motor and between current and angle of the tip are established. The reason for using this representation will be seen clearly in the next section. We just mention here that identifying the transfer function between the angle of the motor and the angle of the tip produces a transfer function that is independent of motor friction. Consequently, nonlinear terms are not present, thus allowing the use of conventional identification frequency methods to obtain the beam dynamics.

III. Robust Control Scheme

A control scheme that reduces the effects of friction is proposed here. This scheme is a modification of the classical high-gain position closed-loop procedure and incorporates a constant feedforward term to remove the remaining steady-state error due to Coulomb friction.

A. General Feedback Control Scheme

The proposed control scheme is shown in Fig. 3. Motor position θ_m and tip position θ_t are controlled by two nested closed loops

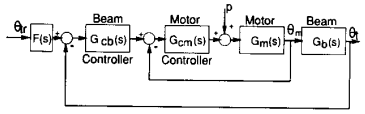

Fig. 3. Proposed general control scheme.

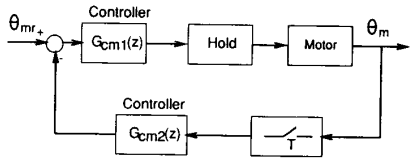

Fig. 4. Inner loop of proposed control scheme.

whose controllers are denoted as $G_{cm}(s)$ and $G_{cb}(s)$. Motor transfer function $G_m(s)$ relates the current to the angle of the motor. $G_b(s)$ is the transfer function of the flexible beam and relates the angle of the motor to the tip angle. $G_b(s)$ has all its poles in the left half-plane but may have (for arms with more than one vibrational mode) some zeros in the right half-plane (nonminimum phase system). The overall transfer function of the arm, which relates the current of the motor to the tip position, $G(s) = G_m(s)G_b(s)$ has no poles in the right half-plane. All the poles and zeros of $G_m(s)$ lie in the left half-plane because its poles are the poles of $G(s)$ and its zeros are the poles of $G_b(s).F(s)$ is a feedforward compensator.

As mentioned earlier, frictional effects may be minimized by using high position feedback gains. However, the gains of a standard pole-placement controller cannot be increased arbitrarily in flexible arms because of the right half-plane zeros. In the proposed scheme, the gains for the inner loop may be increased arbitrarily [using an appropriate controller $G_{cb}(s)$] without making the system unstable, because $G_m(s)$ is minimum phase. So, intuitively, the high-gain inner loop to control the motor position makes the system insensitive to friction and then, a second outer loop may be designed to control the tip position. The outer loop cannot have an arbitrary high gain because $G_b(s)$ is nonminimum phase, but now it does not matter because the effects of friction have been nearly removed by the high-gain inner loop.

It was shown by Rattan *et al.* [15] that the proposed control scheme is less sensitive to friction than the standard pole-placement controller. Signal-to-noise ratio and sensitivity ratio to V were used as sensitivity indices to Coulomb friction and dynamic friction variations, respectively. Analysis showed that the first index may be increased arbitrarily whereas the second may be reduced arbitrarily in this scheme by increasing the gains of the inner controller. These two indices are limited by the stability margins in the gains of the pole-placement controller.

B. Feedforward Term

The preceding scheme overcomes stability problems caused by the implementation of high-gain feedback loops (to increase the robustness to friction) in nonminimum phase systems. However, small steady-state errors may still be present. A feedforward term is added to the current of the motor to remove this error. This term is used to compensate for an ideal Coulomb friction torque, and the value used here is the average value given by the identification method. The sign of the feedback term depends on the sign of the motor velocity.

IV. Design of Inner Loop Controller

The main objective of the inner loop is to remove the modeling errors and the nonlinearities introduced by friction due to very high gains. Another important goal is to make the response of the inner loop significantly faster than the response of the outer loop and, of course, much faster than the motions produced by the vibrational modes of the arm. This simplifies the design of the outer loop. In fact, if the inner loop is relatively fast, we can replace the inner loop of Fig. 3 by a block with unity transfer function. Then, the dynamics of the flexible arm is reduced to $G_b(s)$, and the input is the commanded motor position θ_{mr}.

Three approaches may be used to design the controller of the inner loop provided that a feedforward term is used to compensate for Coulomb friction:

1) Design a regulator to control the linear part of (1), which is minimum phase but may be quite complex even having zeros on the imaginary axis.
2) Design a regulator to control the reduced linear part of (1), where C_t is assumed to be another perturbation:

$$Ki(t) = J\frac{d^2\theta_m(t)}{dt^2} + V\frac{d\theta_m(t)}{dt}. \tag{8}$$

3) Design a regulator to control the system given by (8) but use another feedforward term to compensate for C_t. This coupling torque may be measured directly by a strain gauge installed on the base of the beam, or can be estimated from tip and motor angles.

The third approach was used herein because it simplifies the design of the inner loop controller and because we want to explore the possibilities of estimating the coupling torque from measurements of the motor and tip position. Since the control is robust, only an approximate estimation of this torque is needed. The errors produced by this approximation will be compensated by the high-gain inner loop. These points will be developed and illustrated in the examples of Section VI.

Assuming that we estimate the value of C_t, the system may be approximately decoupled and linearized by adding the following term into the current:

$$i_c(t) = \frac{1}{K}[C_t(t) + C_f(\text{sign of motor velocity})].$$

Then, the motor transfer function, $G_m(s)$, reduces to the typical transfer function of dc motors as

$$\frac{\theta_m(s)}{I(s) - i_c(s)} = \frac{K/J}{s(s + V/J)} = \hat{G}_m(s). \tag{9}$$

A digital controller of the form shown in Fig. 4 can be designed to get a very fast response without an overshoot. This figure represents the inner loop to control the motor position, where $G_{cm1}(z)$ and $G_{cm2}(z)$ are phase-lead controllers. The limits in the gains of $G_{cm1}(z)$ [resembling $G_{cm}(s)$ of Fig. 3] depend on the current limit of the amplifier of the dc motor as well as beam deflection limits. In the cases where the coupling torque is high, it is necessary to take into account in the design the current drained by the coupling compensation term. This will lower the value of the maximum current that is available for the feedback control of Fig. 4.

V. Design of Outer Loop Controller

If friction effects were removed, and the motor response was much faster than the dynamics of the mechanical beam by closing the inner loop, then motor dynamics could be represented by a unity transfer function. This can be done in lightweight flexible arms, but this assumption no longer remains true if the reaction torque of the

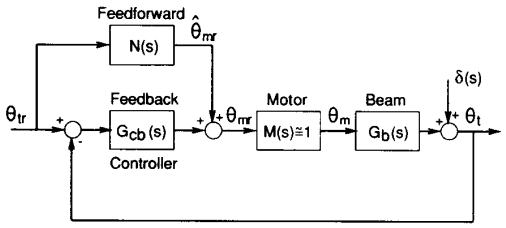

Fig. 5. Feedforward control scheme.

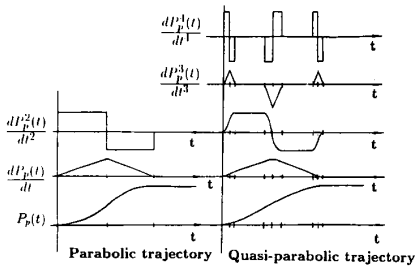

Fig. 6. Parabolic and quasi-parabolic trajectories.

flexible arm is important compared with the motor input torque. In this case, the assumption still can be used as a first approximation in the design of the tip position controller, and correction terms may be added later that compensate for motor delays and residual dynamics. Then, the dynamics of the flexible arm are reduced to $G_b(s)$, that now relates the reference of the motor position with the tip position. This simplifies the design of the tip controller, and relates in an easy way the commanded trajectories with the mechanical limitations of the beam. These two facts suggest that the two nested closed loops scheme proposed here may be interesting even when friction in the joints is not important.

Several approaches were mentioned in the introduction to control the tip position either from state-space or frequency-domain techniques. We used a classical feedback controller combined with a feedforward term (see Fig.. 5). The feedforward term, which generates a control signal $\hat{\theta}_{mr}$, is mainly responsible for driving the motor in such a way that the tip of the arm follows the desired trajectory. If the feedforward term is designed properly, position error between the tip position and its desired trajectory will be small, allowing us to use a very simple feedback controller.

A. Feedforward Term

Let us assume a stable system whose transfer function is $G_b(s)$. Assume that we want its output to follow a nominal trajectory, represented by its Laplace transform $u(s)$, as close as possible minimizing the integral square error (ISE)

$$\text{ISE} = \int_0^\infty e^2(t)dt = \frac{1}{2\pi j}\int_{-j\cdot\infty}^{j\cdot\infty} e(s)e(-s)ds, \qquad (10)$$

where $e(t) = u(t) - \theta_t(t)$. A feedforward term $N(s)$ that minimizes (10) with the constraint of being stable can be determined by the Wiener filter technique [16], [17] as

$$N(s) = \left| \frac{G_b(-s)I_{uu}(s)}{G_b^-(s)I_{uu}^-(s)} \right|_+ / G_b^+(s)I_{uu}^+(s) \qquad (11)$$

where $G_b(s)G_b(-s) = G_b^+(s)G_b^-(s), G_b^+(s)$ and $G_b^-(s)$ group all the poles and zeros of $G_b(s)G_b(-s)$ that are in the left and right half-planes, respectively, and $I_{uu}(s) = u(s)u(-s) = I_{uu}^+(s)I_{uu}^-(s), I_{uu}^+(s)$ and $I_{uu}^-(s)$ group all the poles and zeros of $I_{uu}(s)$ in the left and right half-planes, respectively. Also,

$$\frac{G_b(-s)I_{uu}(s)}{G_b^-(s)I_{uu}^-(s)} = \left| \frac{G_b(-s)I_{uu}(s)}{G_b^-(s)I_{uu}^-(s)} \right|_+ + \left| \frac{G_b(-s)I_{uu}(s)}{G_b^-(s)I_{uu}^-(s)} \right|_-$$

where assuming that the partial fraction expansion of the left-hand side of the preceding equation has been done, the + subscript represents the grouping of the fractions corresponding to the roots placed in the left half-plane and the − subscript represents the grouping of the ones corresponding to the roots in the right half-plane. Notice that if $G_b(s)$ is minimum phase, then $N(s) = G_b^{-1}(s)$.

B. Trajectories

Robot trajectories must be simple enough to be generated in real time and to allow a real-time generation of the feedforward control signal and must take into account the physical limitations on the mechanical structure. The simplest trajectories that fulfill this are the parabolic trajectories used for rigid arms. These trajectories can also be utilized for minimum phase flexible arms but not for nonminimum phase flexible arms because the corresponding feedforward signal is unbounded [17]. Quasi-parabolic trajectories are utilized in this case (see Fig. 6), which are very similar to parabolic trajectories but have bounded derivatives up to fourth order. Their acceleration profile is the same as the parabolic trajectories with a slight rounding in the corners. Thus the quasi-parabolic trajectories behave most of the time as parabolic, except during very small intervals of time that correspond to changes in the acceleration.

C. Feedback Controller

The feedback controller is designed using classical frequency-domain techniques. The function of this controller is to compensate for the deviation of the tip position from the desired trajectory. To move the arm to the desired angle, most of the control action required is provided by the feedforward term. When the arm is not moving and an external disturbance produces a deviation from the reference position, the controller G_{cb} provides a control action to recover the desired position. Thus, the controller compensates only for small deviations, and we can use high gains (when the system is minimum phase) without saturating the amplifier of the motor. This improves the dynamic performances of the controlled system significantly. A PID controller is proposed to remove permanent errors caused by an imperfect compensation of Coulomb friction.

VI. Experimental Results

Methods described herein are applied to a class of flexible arms that we have built in our laboratory. Two very lightweight and slender arms were designed. Because beam torques were low, problems related with joint friction became important. Identification and control of single-degree-of-freedom flexible arms with friction in the joints are developed for minimum and nonminimum phase cases.

A. Experimental Setup

The mechanical system consists of a dc motor, a slender arm attached to the motor hub, and a mass at the end of the arm floating on an air table. Fig. 7 shows the major parts of the system, and Fig. 8 shows the mechanical structure of the two arms. The arm is a piece of music wire (7 in long and 0.032 in in diameter) clamped in the motor hub. The tip mass is a 1/16-in-thick, 5 3/4-in diam fiberglass disk attached at its center to the end of the beam with a freely pivoted pin joint. The disk has a mass of 55 g and floats on the horizontal

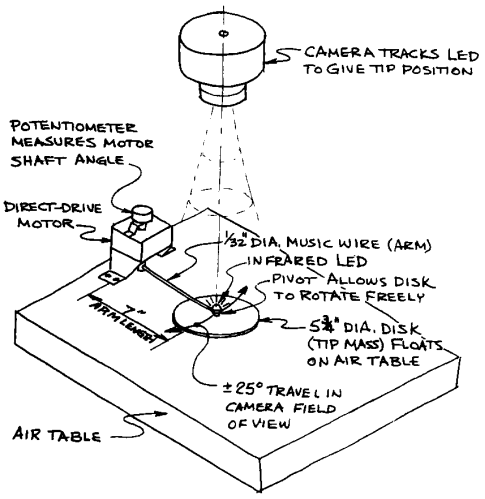

Fig. 7. Experimental setup.

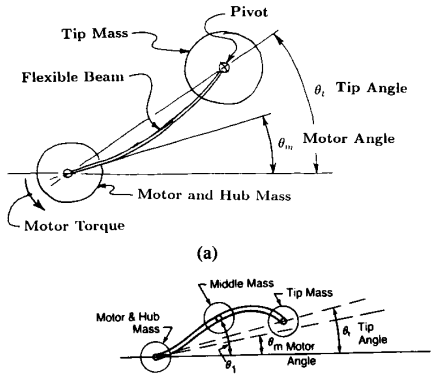

Fig. 8. (a) Single-mass and (b) two-mass flexible arms.

air table with minimal friction. Since the mass of the beam is small compared with that of the disk and because the pinned joint prevents the generation of a torque at the end of the beam, the mechanical system used for the first example behaves practically like an ideal, undamped mass-spring system (a minimum phase system). In the second example, the wire is replaced by a longer one and two free pinned masses are attached, one at the middle and the other at the end of the wire. The second system has the characteristics of flexible arms with distributed mass, and is a nonminimum phase system.

An inland direct-drive motor drives the arm. The amplifier current limit is set to 4.12 A, which corresponds to 9.0 lb · in motor torque. Static friction of the motor is about 0.288 lb · in (0.132 A) and has a significant effect on the control when the torque of the arm is low. Two sensors are used for the control of the system. A 7/8-in, 360°potentiometer provides the angle of the motor shaft. A Hamamatsu tracking camera senses the x-y position of an infrared LED mounted on the tip of the arm. The control algorithm is implemented on a Omnybyte OB68K1A, MC 68000-based computer with 512K bytes dynamic RAM and 10-MHz clock. Since the control computer is relatively slow, real computations are done in integer or short integer mode. Analog interfacing is provided with 12-bit A/D and D/A boards.

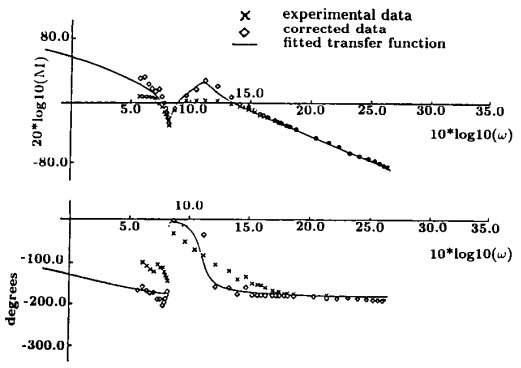

Fig. 9. Frequency data for identification of motor dynamics (single mass).

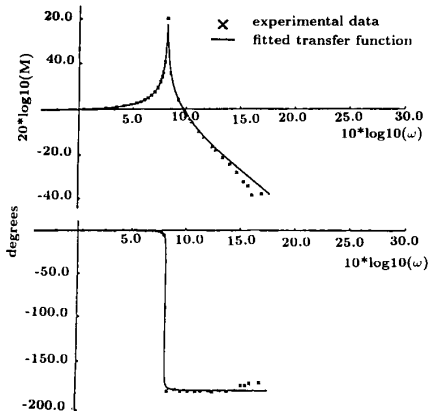

Fig. 10. Frequency data for identification of beam dynamics (single mass).

B. Single-Mass Flexible Beam

1) Identification: Using the identification scheme explained in Section II, we get the frequency plots shown in Fig. 9 and 10. Fig. 9 shows the magnitude and phase characteristics of the motor. Experimental data are represented by crosses, and corrected data [obtained from processing the experimental data using (7) where the Coulomb friction C_f is estimated from the method described in Subsection II.B] is represented by diamonds. Notice that our method has allowed us to reconstruct a resonant peak due to the coupling between the motor and the beam. This peak cannot be characterized from the experimental data obtained by using the classical method, and is hidden due to Coulomb friction. Fig. 10 shows the characteristics of the beam. It is very close to the expected model of an ideal minimum phase flexible beam without mass in the wire and with only one vibrational mode.

Transfer functions are fitted to the corrected data of Fig. 9 and the data of Fig. 10 using a maximum likelihood estimation algorithm. They are given by

$$G_m(s) = \frac{394.94(s^2 + 0.06s + 43.75)}{s(s^3 + 2.26s^2 + 165.7s + 103.56)} \tag{12}$$

$$G_b(s) = \frac{43.75}{s^2 + 0.06s + 43.75}. \tag{13}$$

In this arm $C_t = C(\theta_m - \theta_t)$ and, from the linear part of (1), we get the following motor coefficients: $J = 0.005529$ lb · in · s^2, $V = 0.01216$ lb · in/rad/s, $C = 0.674$ lb · in/rad, and $K = 2.184$

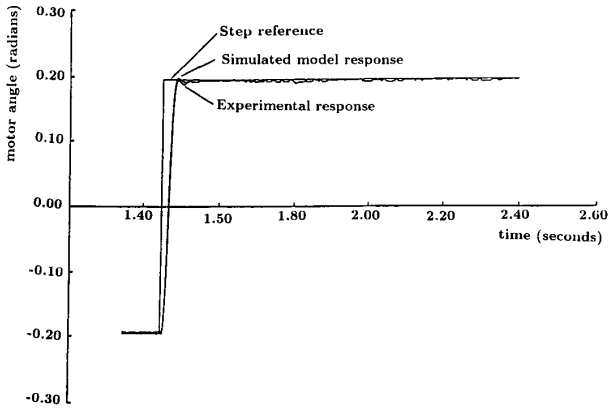

Fig. 11. Theoretical and experimental step responses of inner loop (single mass).

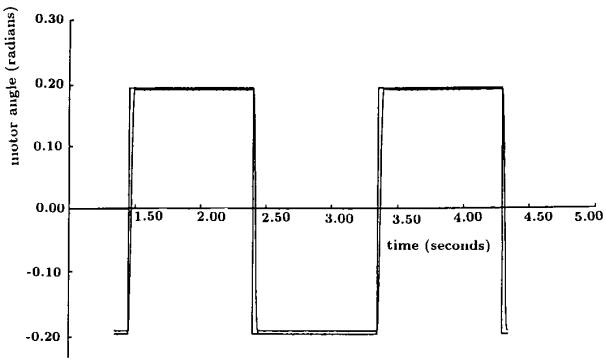

Fig. 12. Experimental step response of inner loop (without Coulomb friction compensation).

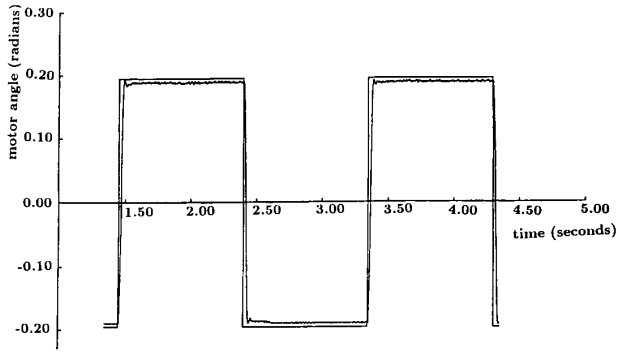

Fig. 13. Experimental step response of inner loop (without coupling torque compensation).

lb · in/A (this last value obtained from catalog). The value of the Coulomb friction estimated by the method of Section II is 0.132 A. This corresponds to an equivalent torque generated by a deflection of the beam of 25°, so its effect is very noticeable. Coefficients of the identified $G_b(s)$ are very close to the coefficients obtained analytically from the mechanical equations of the beam, confirming the assumption that there is no distributed mass and the arm is a minimum phase system.

2) Inner Loop Control design: The parameters estimated in the preceding subsection are used to design the controllers of Fig. 4 and to implement the feedforward terms (coupling torque of this arm is proportional to C times the difference between the motor and tip angles). A sampling period of 3 ms is used, and a delay of one sampling period caused by real-time computations has been assumed.

An optimization program was developed to get the best controllers $G_{cm1}(z)$ and $G_{cm2}(z)$ using the model obtained for the motor. The settling time of the response of the motor loop to step commands was minimized. Step inputs were assumed because θ_{mr} should experience very sharp changes if quick tip motions are desired. The following constraints were used in the design: $G_{cm2}(1) = 1$ to guarantee the zero steady-state error of the response and $G_{cm1}(1) = 15$ to limit the peak of the current of the motor (a step of amplitude 400 mrad should produce a peak of 6 A).

The response of the controlled motor to step commands was obtained keeping the tip of the arm fixed in the zero position. There is a coupling torque in the steady state of this experiment caused by a bending of 200 mrad (difference between the motor and tip angles in the steady state). Fig. 11 compares simulated and experimental responses. Both responses are very close and demonstrate the accuracy of the parameters estimated in the preceding subsection. The zero steady-state error shown by the experimental data demonstrates the effectiveness of the compensation achieved for Coulomb friction and coupling torque. The settling time of the motor is 33 ms, which is significantly faster than the dynamics of the beam and allows us to neglect inner loop dynamics. Figs. 12 and 13 show the responses when the friction and decoupling compensators are removed, respectively. These figures show that these compensators do not improve the transient response but eliminate the steady-state error.

3) Outer Loop Control Design: Equation (13) shows that $G_b(s)$ is minimum phase. Then $N(s) = G_b^{-1}(s)$ and parabolic references are used. Maximum acceleration is proportional to the maximum beam torque, which is proportional in this arm to the deflection. It is easy to show that deflection = acceleration/43.75. The maximum allowed deflection is 400 mrad (23°) and, therefore, the maximum acceleration is 8750 mrad/s^2. We have assumed a deflection of 200 mrad (50% of the maximum deflection) to calculate this acceleration to allow some extra deflection for the action of the controller $G_{cm1}(s)$.

A discrete PID controller was used for $G_{cb}(z)$, whose parameters were optimized to minimize the time needed by the arm to recover its desired position when changes in the position were produced by external perturbations. This controller was

$$G_{cb} = 100\frac{(1 - 0.98z^{-1})(1 - 0.99z^{-1})}{(1 - z^{-1})(1 - 0.61z^{-1})}.$$

Fig. 14 shows the tip response of the parabolic profile. The settling time is 0.22 s. A comparison between the angle of the tip and the angle of the motor is given in Fig. 15, which shows that the dynamics of the inner loop is much faster than the outer loop and the movements required are larger.

C. Two-Mass Flexible Arm

This arm was built to test our control scheme with a nonminimum phase flexible arm of several vibrational modes. It consists of a piece of music wire (stiffer than the one used in the previous experiment) with two masses attached: one concentrated mass in the middle of the beam and the other at the tip. The masses are free pinned disks that float on an air table. This arm presents dynamic characteristics similar to the ones of flexible arms with distributed mass, although it exhibits only two modes of vibration.

1) Modeling and Identification: Only beam dynamics have to be characterized because the motor is the same as before. Earlier

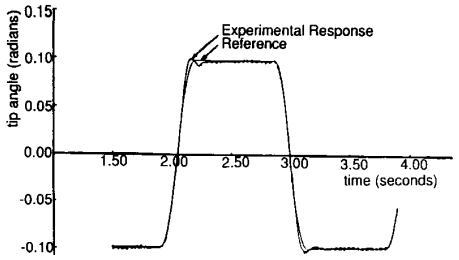

Fig. 14. Tip response of single-mass arm.

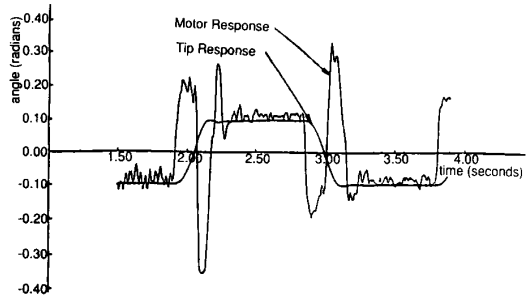

Fig. 15. Tip and motor responses of single-mass arm.

identification showed a good agreement between theoretical and experimental beam transfer functions. Then the transfer function of the two-mass arm is calculated analytically from the stiffness and dimensions of the beam and the masses of the disks:

$$\frac{\theta_t(s)}{\theta_m(s)} = \frac{-45.475(s^2 - 1273.3)}{s^4 + 1637.1s^2 + 57903.3175}, \tag{14}$$

and the coupling torque can also be obtained from mechanical analysis as

$$C_t(s) = 2.05274\frac{1591.625 + 2s^2}{1682.575 + s^2}(\theta_m(s) - \theta_t(s)). \tag{15}$$

2) Inner Loop Control Design: The motor of the first arm is used here so that the Coulomb friction compensation remains the same. Compensators $G_{cm1}(z)$ and $G_{cm2}(z)$ are the same too. But the decoupling term is more complex. A transfer function that relates C_t with the difference between the motor and tip angles can be found by combining (14) and (15). But it has two imaginary poles that produce undesired oscillations and instability when implemented on a computer. Instead, we use a simple approach that cancels only steady-state values of C_t:

$$\hat{C}_t(t) = 1.941(\theta_m(t) - \theta_t(t)). \tag{16}$$

The experiment of Subsection VI.B.2 was repeated. Fig. 16 represents the experimental response of the controlled motor and shows that the inner loop dynamics is still significantly faster than beam dynamics (the settling time for the 5% position error is about 60 ms) despite considerably more inertia. It also shows that the steady-state errors are small, but there is a small ripple caused by the compensator (16), which does not compensate high-frequency coupling dynamics. Fig. 17 shows the response without the decoupling compensator which has a nonzero steady-state error. Note that this term does not affect the temporal response of the motor [probably because of the high gains used in the controller $G_{cm1}(z)$] but nearly removes steady-state errors caused by the coupling torque C_t.

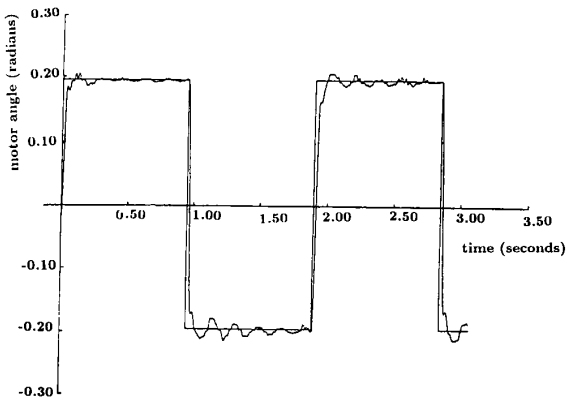

Fig. 16. Experimental step response of inner loop (two-mass arm).

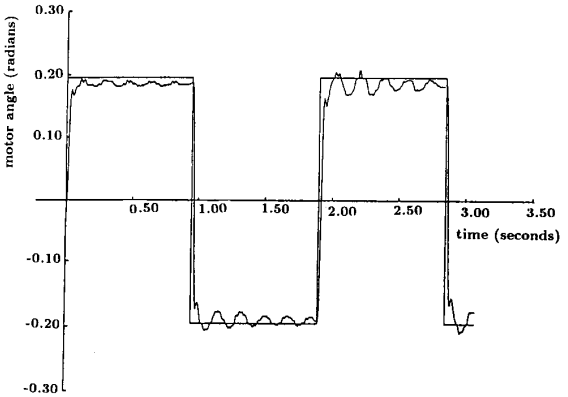

Fig. 17. Step response of the inner loop without motor-beam decoupling (two-mass arm).

3) Outer Loop Control Design: A quasi-parabolic reference was used whose parameters were chosen taking into account the maximum allowable deflection of the beam: acceleration = 7875 mrad/s^2; second derivative of acceleration = 8 648 646 mrad/s^4.$N(s)$ was obtained from (11) as

$$N(s) = (s^4 + 1637.1s^2 + 57903.7175) \cdot \frac{1 + 0.05605s + 0.00157075s^2}{45.475(s + 35.68333)^2}.$$

A simple discrete PD feedback controller was used. Fig. 18 shows the tip response to the quasi-parabolic profile, and Fig. 19 compares the motor and tip angles. Notice that the first vibrational mode has been removed, and the second one has been reduced to a small damped ripple whose maximum amplitude is less than 3% of the step amplitude. The settling time is 0.3 s. The effective compensation of Coulomb friction and static coupling torque carried out in the inner loop removed permanent errors and made unnecessary the use of a PID controller.

VII. Conclusion

This paper studied the control of flexible arms with friction in the joints. New methods for their identification and control have been proposed. The approach is based on classical control theory, using transfer functions and simple frequency-domain methods, in contrast

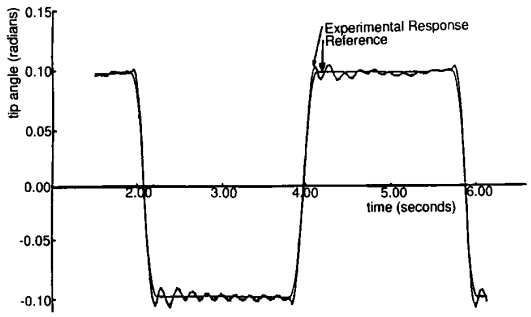

Fig. 18. Tip response of two-mass arm.

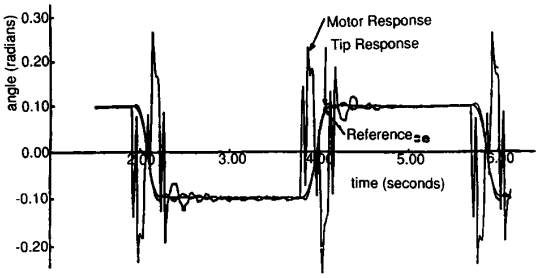

Fig. 19. Motor and tip position responses of two-mass arm.

to most of the work done on flexible arms that is based on state-space models, and pole assignment or optimization methods.

The proposed identification method extends frequency-domain techniques for linear systems to systems with Coulomb friction, which is a strong nonlinearity. The method identifies the linear part of the model and gives an estimation of the Coulomb friction. This presents two advantages: 1) Coulomb friction is estimated for the normal range of velocities at which the arm is operating, whereas other methods estimate Coulomb friction by extrapolating high-speed measurements, since the constant-speed regime at low velocities cannot be maintained because of stiction; 2) it gives an average value of the Coulomb friction over a continuous range of velocities, whereas other methods determine friction only at some speeds and then average these values [13]. All this has been done under the assumption of Coulomb friction, and it is a reasonable approach in many cases. For nonideal friction, this method gives an averaged value.

The classical method of closing a high-gain position feedback loop to reduce the effects of friction in rigid arms has been modified to include nonminimum phase flexible arms. Two nested loops are designed: an inner loop that considers the dynamics of the motor (a compensator is used to decouple the motor from the beam) and an outer loop that considers the dynamics of the flexible beam. The inner control loop is designed by any standard method; the outer loop combines feedforward and feedback control techniques to drive the arm without tip oscillations.

The proposed control scheme was applied to a class of very slender flexible arms. In these arms frictional torque was of the same order of magnitude as motor-beam coupling torque. Thus the effects of friction are important and should be considered. The method was applied to minimum and nonminimum phase arms, giving simple controllers that provide fast and precise motion of the tip. Notice that the limit for the speed of motion was given by the maximum allowable deflection of the beam, which in these arms is a more restrictive condition than the design condition of the outer loop bandwidth to be significantly smaller than the actuator bandwidth.

The control scheme is general and can be applied to heavier flexible arms. However, in heavier arms, the current needed to compensate for the coupling between the motor and the beam may be large, and the assumption of negligible inner loop dynamics no longer remains true (a first-order model of the heavier arm usually gives a good approximation). Finally, we mention that this control scheme has also been used in multilink flexible arms [18].

VIII. References

[1] R. H. Cannon and E. Schmitz, "Precise control of flexible manipulators," *Robotics Research,* 1985.

[2] F. Matsuno, S. Fukushima, and coworkers, "Feedback control of a flexible manipulator with a parallel drive mechanism," *Int. J. Robotics Research,* vol. 6, no. 4, Winter 1987.

[3] F. Harahima and T. Ueshiba, "Adaptive control of flexible arm using end-point position sensing," in *Proc. Japan-USA Symp. Flexible Automation,* Osaka, Japan, July 1986.

[4] B. Siciliano, B. S. Yuan, and W. J. Book, "Model reference adaptive control of a one link flexible arm," in *Proc. 25th IEEE Conf. Decision and Contr.*, Athens, Greece, Dec. 1986.

[5] D. M. Rovner and R. H. Cannon, "Experiments towards on-line identification and control of a very flexible one-link manipulator," *Int. J. Robotics Research,* vol. 6, no. 4, Winter 1987.

[6] J. C. Ower and J. Van de Vegte, "Classical control design for a flexible-manipulator: Modeling and control system design," *IEEE J. Robotics and Automation,* vol. RA-3, no. 5, Oct. 1987.

[7] B. C. Kuo, *Automatic Control Systems.* Englewood Cliffs, NJ: Prentice-Hall, 1982.

[8] C. Wu and P. Paul, "Manipulator compliance based on joint torque control," in *Proc. 9th IEEE Conf. Decision and Control* 1980.

[9] M. Handlykken and T. Turner, "Control system analysis and synthesis for a six degree-of-freedom universal force reflecting hand controller," in *Proc. 9th IEEE Conf. Decision and Control,* 1980.

[10] C. D. Walrath, "Adaptive gearing friction compensation based on recent knowledge of dynamic friction," *Automatica,* vol. 20, 1984.

[11] C. Canudas, K. J. Astrom, and K. Braun, "Adaptive friction compensation in DC-motor drives," *IEEE J. Robotics and Automation,* vol. RA-3, no. 6, Dec. 1987.

[12] G. G. Hastings and W. J. Book, "Verification of a linear dynamic model for flexible robotic manipulators," in *Proc. 1986 Int. Conf. on Robotics and Automation,* San Francisco, CA, Apr. 1986.

[13] V. Feliu, K. S. Rattan, and H. B. Brown, "Model identification of a single-link flexible manipulator in the presence of friction," in *Proc. 19th Annual Modeling and Simulation Conf.,* Pittsburgh, PA, May 1988.

[14] A. V. Oppenheim and R. W. Schafer, *Digital Signal Processing.* Englewood Cliffs, NJ: Prentice-Hall, 1975.

[15] K. S. Rattan, V. Feliu, and H. B. Brown, "A robust control scheme for flexible arms with friction in the joints," in *Proc. 1988 NASA-Air Force Workshop Space Operations Automation and Robotics,* Dayton, OH, July 1988.

[16] S. C. Gupta and L. Hasdorf, *Fundamentals of Automatic Control.* New York: Wiley, 1970.

[17] V. Feliu, K. S. Rattan, and H. B. Brown, "Modelling and control of single-link flexible arms with lumped masses," *ASME J. Dyn. Syst., Meas., Contr.,* vol. 114, Mar. 1992.

[18] V. Feliu, K. S. Rattan, and H. B. Brown, "Design and control of a two-degree-of freedom lightweight flexible arm," *Proc. 30th IEEE Conf. Decision and Control,* Brighton, England, Dec. 1991.